Sodium overlayers on low-index tungsten surfaces: Field and photofield emission currents and surface electronic structures

Z. A. Ibrahim* and M. J. G. Lee†

Department of Physics, University of Toronto, 60 St. George Street, Toronto, Ontario, Canada M5S 1A7

(Received 10 September 2010; revised manuscript received 13 February 2011; published 21 April 2011)

The total-energy distributions (TEDs) of the emission currents in field emission and surface photofield emission and the overlayer-induced modifications in the surface electronic structures from the technologically important W surfaces with the commensurate W(100)/Na $c(2 \times 2)$ and W(110)/Na (2×2) overlayers are studied from first principle and compared to experiments. The TEDs obtained by our recent numerical method that extends the full-potential linear augmented plane-wave method for the electronic structures to the study of field and photofield emission are used to interpret the shifts of the peaks in the experimental TEDs in field emission and photofield emission from the W(100) and W(110) surfaces at submonolayer and monolayer Na coverage. Wave function overlap of the 3*s* Na states and the pairs of d_{z^2}-like surface states of the strong Swanson hump in clean W(100) below the Fermi energy shifts these W states by about -1.2 eV, thus stabilizing these states, to yield new strong peaks in the TEDs in field emission and photofield emission from W(100)/Na $c(2 \times 2)$, in agreement with experiments. Na intralayer interactions shift the strong *s*- and *p*-like peaks in the surface density of states of W(110) below and above the Fermi energy, respectively, to lower energy with increasing coverage.

DOI: 10.1103/PhysRevB.83.165430 PACS number(s): 73.20.At, 73.30.+y, 79.70.+q, 82.45.Mp

I. INTRODUCTION

Field emission is extensively used in technological applications for imaging as well as to study the electronic properties at metal and semiconductor surfaces and thin-film overlayers.[1,2] Modifications in the electron emission characteristics of transition metals due to the adsorption of alkali-metal overlayers and their oxides is of great interest both fundamentally and technologically.[3] The reduction in the work function, induced by the overlayer, enhances the quantum-mechanical tunneling of electrons through the surface, making these interfaces suitable for thermionic cathode and photoelectron emission device applications. To understand and improve the performance of these devices, it is important to microscopically interpret the physical mechanisms at the interfaces that modify the electronic structures and emission current with changing coverage. Details of the theoretically extracted electronic structure are expected to shed light on the role played by surface states and surface resonances in the substrate—overlayer bonding, the nature of bonds formed, the charge shifts, and modification of the potential induced at the interface by the overlayer. While several such overlayer systems have been extensively studied theoretically,[4–6] work on the tungsten-sodium (W-Na) interface has been limited to only the (100) plane,[3] or was using simplified formalisms that neglect the dependence of the substrate electronic structure on surface orientation.[7,8]

Most experimental studies of the W-Na interfaces were focused on work-function measurements and understanding the Na growth mechanism.[3,9–12] Photoemission measurements[13] from W(110) covered by Na, K, and Cs from low up to complete one-monolayer coverage were used to analyze the binding energies of the alkali *s*, and tungsten 3*p* and 4*f* core electrons. Metastable impact electron spectroscopy and ultraviolet photoemission spectroscopy were used to study the electron spectra from Li, Na, K, and Cs overlayers on W(110).[14] An experimental investigation of the valence electronic structure of the W-Na-vacuum interfaces for W(100) and W(110) was carried out by Derraa and Lee[15] by the surface sensitive field emission (FE) and photofield emission (PFE) techniques. Na coverage was in the range $\theta = 0$ to $1/2$ and $\theta = 0$ to $1/4$, respectively, where θ is the ratio between the number of atoms in the overlayer and that in the outermost substrate layer.

Although many experimental results on W-Na have been available for more than a decade and in spite of the technological importance of these interfaces, only a few theoretical investigations—including only one recent[3] parameter-free, *ab initio* study—of the electronic structure of these interfaces are reported. The recent work[3] on Na overlayer growth at W electrodes in high-pressure Na discharge lamps discusses the Na pressure-dependent work function at the W(100) surface at different coverages. The measured work function was compared with results of electronic structure calculations of W(100) with commensurate Na overlayers at different coverage using the pseudopotential plane-wave method based on density-functional theory (DFT). Lang[7] carried out surface electronic structure calculations of a metal surface with a single Na atom, and Ishida[8] calculated the electronic structure at different Na coverage, both applying the jellium model to the substrate. These results[7,8] were used in Ref. 15 to interpret the experimental FE and PFE data. The low-index surfaces of W, however, contain several *d*-like surface states and surface resonances[16,17] that are crucial for the understanding of the substrate-overlayer bonding, and which the jellium model is unable to accurately describe.

In the present paper, we report the modifications in the surface electronic structures of W(100) and W(110) substrates due to commensurate Na overlayers using the *ab initio* full-potential linear augmented plane-wave (FP-LAPW) method in order to interpret the existing experimental FE and PFE data.[15] FE and PFE are very sensitive to the electronic states close to $\bar{\Gamma}$, the center of the surface Brillouin zone (SBZ), because the surface potential barrier attenuates exponentially the electronic states of increasing wave vector. To accurately

compare the theoretical results with the experiments we extend the electronic structure calculations to yield the total-energy distributions (TEDs) of the emission currents in FE and surface PFE and the *k*-resolved layer densities of states.

Low-energy electron-diffraction (LEED) measurements[11] demonstrate that Na from an atomic beam grows pseudomorphically layer by layer on W(100)/Na up to 80 layers in a $c(2\times 2)$ structure corresponding to $\theta = 1/2$. Our W(100) calculations were carried out with a Na $c(2\times 2)$ overlayer [denoted W(100)/Na $c(2\times 2)$], which corresponds to one monolayer (ML) coverage. On W(110), LEED data[10] show that the Na overlayer undergoes a number of successive commensurate structures before completing the first atomic ML, which is an incommensurate, hexagonal layer at a coverage corresponding to $\theta = 3/5$. Since our numerical method, based on the repeated slab geometry, involves the assumption of translational symmetry parallel to the surface, only commensurate overlayers were considered. We carried out emission current calculations at a commensurate overlayer corresponding to $\theta = 1/4$ [denoted W(110)/Na ($S_{1/4}$), *S* stands for structure], which represents a (2×2) overlayer observed in the LEED data,[10] in order to compare them with available experimental results.[15] To study the modification of the electronic structure with increased Na concentration we also report results with overlayers at $\theta = 2/5$ [W(110)/Na ($S_{2/5}$)] and $\theta = 1/6$ [W(110)/Na ($S_{1/6}$)], which are the commensurate overlayers of highest and lowest density respectively observed by the LEED measurements.

In Sec. II of this paper details of the electronic structure calculations are reported. In Sec. III the results of the electronic structure calculations and TEDs of the W(100)/Na $c(2\times 2)$ are interpreted and compared to the experimentally measured TEDs in FE and PFE. Similar discussions of W(110)/Na ($S_{2/5}$), W(110)/Na ($S_{1/4}$), and W(110)/Na ($S_{1/6}$) follow in Sec. IV. The results and conclusions of this work are summarized in Sec. V.

II. COMPUTATIONAL METHODS

The metal-adsorbate-vacuum interface is represented by the periodically repeated supercell partially filled with the metal and adsorbate atoms followed along the *z* direction by a region of vacuum. The electronic structure of the supercell is calculated self-consistently on the basis of DFT by the FP-LAPW method using the electronic structure software package WIEN2K.[18] The wave function is expanded in terms of radial functions multiplied by spherical harmonics close to the atoms and in terms of plane waves in the interstitial regions, which facilitates the breaking up of the electronic properties into their partial angular momentum components *s*, *p*, and *d*. Exchange and correlation are treated in the generalized-gradient approximation.[19] Core states are treated fully relativistically[20] and for valence states spin-orbit effects are incorporated via a second variational procedure using the scalar relativistic eigenstates as basis.[21–23] Spin-orbit interactions have been included in all calculations except those for W(110)/Na ($S_{1/6}$) that are highly central processing unit demanding due to the large supercell. To calculate the TEDs in FE and surface PFE and the ***k***-resolved surface density of states (*K*-SDOS) we modified the software package WIEN2K as described below and in more detail in Refs. 16 and 17.

In FE, an interface plane of the crystal is defined outside the surface beyond which the electric field is effective. In the interface plane, the potential energy varies only weakly therefore the wave function $\psi_{\mathbf{k}}(\mathbf{r})$ of wave vector $\mathbf{k} = (\mathbf{k}_{||}, k_z)$ can be expanded as

$$\psi_{\mathbf{k}}(\mathbf{r}) = \sum_{\mathbf{G}_{||}} A_{\mathbf{k},\mathbf{G}_{||}} \exp[i(\mathbf{k}_{||} + \mathbf{G}_{||})\cdot \mathbf{r}, \tag{1}$$

where $\mathbf{G}_{||}$ are the surface reciprocal-lattice vectors. The zero expansion coefficients $A_{\mathbf{k},0}$ can be evaluated from

$$A_{\mathbf{k},0} = S^{-1}\int \psi_{\mathbf{k}}(\mathbf{r}) e^{-i(\mathbf{k}_{||}\cdot\mathbf{r}_{||})} d\mathbf{S}, \tag{2}$$

where the integration is over a lattice cell of area S in the interface plane. Since the FE current is dominated by states that are close to $\bar{\Gamma}(\mathbf{k}_{||} = 0)$ and by the zero-order ($\mathbf{G}_{||} = 0$) component in the plane-wave expansion, it is an excellent approximation to consider only the contribution of the $\mathbf{G}_{||} = 0$ component to the FE current.[24] The contribution of the electron state $\mathbf{k}$ to the $\mathbf{G}_{||} = 0$ component of the layer density of states (LDOS) divided by the contribution of state $\mathbf{k}$ to the LDOS including all higher components is denoted as the ratio $F_{\mathbf{k}}$:

$$F_{\mathbf{k}} = \frac{A^*_{\mathbf{k},0} A_{\mathbf{k},0}}{S^{-1}\int \psi_{\mathbf{k}}(\mathbf{r})^* \psi_{\mathbf{k}}(\mathbf{r}) d\mathbf{S}}. \tag{3}$$

The highly accurate tetrahedron method of Brillouin-zone integration is used to calculate the surface density of states $\mathrm{SDOS}(E) = \sum_\kappa \sum_i \mathrm{SDOS}_{\kappa,i}(E)$, where *i* and κ are the band index and tetrahedron index, respectively. We modified the software routines to calculate the total-energy distribution of the FE current $j_s(E)$ as follows:

$$j_s(E) = 2ef(E)\sum_\kappa \sum_i F_{\kappa,i}\mathrm{SDOS}_{\kappa,i}(E) v(W_{\kappa,i}) D(W_{\kappa,i}), \tag{4}$$

where *e* is the electron charge, $f(E)$ is the Fermi-Dirac distribution function, *v* is the normal velocity, and the factor 2 takes into account the electron spin. $F_{\kappa,i}\ \mathrm{SDOS}_{\kappa,i}(E)$ is the contribution of band *i* in tetrahedron κ to the $\mathbf{G}_{||} = 0$ component of the LDOS in the interface plane. $D(W_{\kappa,i})$ is the transmission coefficient of the surface potential barrier at normal energy $W_{\kappa,i}$, calculated as the ratio of the charge fluxes on the two sides of the barrier as deduced from the Wronskian of the normal wave function. More details are given in Refs. 16 and 17.

The wave functions of $p_x + p_y$-, $d_{xz} + d_{yz}$-, $d_{x^2-y^2}$-, and d_{xy}-like states at $\bar{\Gamma}$ have a nodal plane perpendicular to the surface, so $A_{\mathbf{k},0}$ vanishes according to Eq. (2). Hence these states do not contribute significantly to FE. On the other hand, $A_{\mathbf{k},0}$ is nonvanishing for the wave functions of *s*-, p_z-, and d_{z^2}-like states at $\bar{\Gamma}$ that lack a nodal plane perpendicular to the surface, causing these states to contribute significantly to FE.

If electrons are excited by surface photoexcitation in *p* polarization, the final states are a continuum of free-electron-like states just outside the surface, and any features in the TEDs in PFE correspond to the initial states of the optical

transition. If the beam is also partially *s* polarized, direct optical transitions are induced by bulk photoexcitation between the initial and final states inside the metal. Hence any observed features correspond to both the initial and final states and will appear at the same final-state energy, irrespective of photon energy $\hbar\omega$. We limited our PFE calculations to surface photoexcitation, which might underestimate the strengths of some peaks that are predominantly due to bulk photoexcitation. The probability of surface photoexcitation from initial state $\mathbf{k}$ is given, apart from an energy-independent prefactor, by $[W_k(W_k+\hbar\omega)]^{-1/2}|M|^2$, where M is an electric-field-dependent optical matrix element.[25] $|M|^2$ varies by only about 1% over the range of electric fields in the present experiments, and this small variation is neglected in the present calculations. We modified the WIEN2K software routines to calculate the TED in surface PFE at final-state energy E by evaluating

$$j(E) \propto f(E-\hbar\omega)\sum_{\kappa}\sum_{i} F_{\kappa,i}\mathrm{SDOS}_{\kappa,i}(E-\hbar\omega) \times \frac{|M|^2}{[W_{\kappa,i}(W_{\kappa,i}+\hbar\omega)]^{1/2}} v(W_{\kappa,i}+\hbar\omega)D(W_{\kappa,i}+\hbar\omega). \quad (5)$$

Finally, K-SDOS(E) was calculated from

$$K-\mathrm{SDOS}(E) = \sum_{\kappa}\sum_{i}\mathrm{SDOS}_{\kappa,i}(E)D(W_{\kappa,i})/D(E). \quad (6)$$

K-SDOS describes the SDOS weighted by the normalized tunneling factor hence emphasizing the energies and symmetries of features in the SDOS in the vicinity of $\bar{\Gamma}$. It involves only contributions from the surface, the region in real space predominantly probed by FE. K-SDOS is independent on the k direction. To identify the states close to $\bar{\Gamma}$ that dominate FE as well as states in a wider region in $\mathbf{k}$ space that strongly contribute to surface PFE and those involved in direct transitions in bulk photoexcitation, it is useful to combine band energy diagrams with the K-SDOS.

Our surface electronic structure calculations of clean W(100) and W(110) using different numbers of W layers in the supercell showed that 13 W layers ensures good convergence.[16] The supercells describing the W(100)/Na $c(2\times2)$ interface and the different W(110)/Na interfaces therefore consist of 13 W layers stacked parallel to the (100) and (110) plane respectively surrounded on each side by a vacuum region of half that volume containing one Na atom. The vacuum region should be thick enough in order to minimize spurious coupling between states in adjacent cells. We have checked the convergence of the potential energy with respect to the thickness of the vacuum region and concluded that a thickness of 19 and 27 Å in the cases of W(100)/Na and W(110)/Na, respectively, used in our simulations, are sufficient. In Fig. 1, the primitive unit cells and corresponding SBZs of the clean substrates and overlayers of W(100)/Na $c(2\times2)$ and W(110)/Na ($S_{1/4}$) are shown.

In this paper, the experimentally observed emission peaks are labeled alphabetically and the emitting facet is denoted by a numerical subscript ("1" for 100 and "2" for 110). The calculated peaks are denoted by a prime. All energies are expressed relative to the Fermi level E_F.

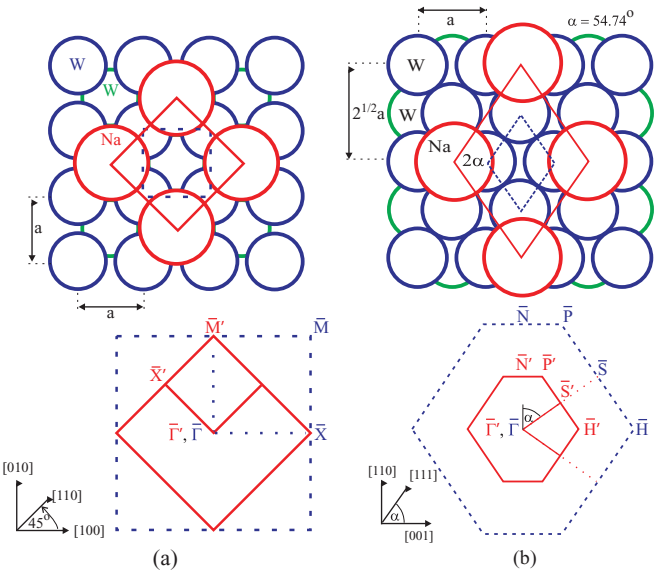

FIG. 1. (Color online) Surface unit cells and surface Brillouin zones (a) of clean W(100) and of a Na $c(2\times2)$ overlayer on W(100) and (b) of clean W(110) and of a Na ($S_{1/4}$) overlayer on W(110). Upper plots: Atomic positions in the overlayer and the next two W layers. Also shown are the primitive unit cells of the clean substrate (blue dashed lines) and of the overlayer (red solid lines). Lower plots: The surface Brillouin zone of the substrate (blue dashed lines) and the overlayer (red solid lines) plotted in the correct orientation relative to the unit cells.

III. RESULTS AND DISCUSSION FOR W(100)/Na

A. Field and photofield emission currents from W(100)/Na $c(2\times2)$

The logarithms of the calculated and the experimental[15] TEDs of the PFE current from W(100)/Na $c(2\times2)$ at room temperature as a function of the initial-state energy are shown in Figs. 2(d) and 2(e) (upper curve at 1-ML coverage), respectively. In our calculations the energy of the photons in a p-polarized beam was 3.05 eV and the electric field strength was 0.16 V Å^{-1} as determined from the experiments. The normal distance between the plane of the Na overlayer and the interface plane was taken to be 1.48 Å. The energies of the peaks are compared in Table I, and the symmetries of the calculated electron states that dominate the emission are reported.

Clean W(100) shows a strong peak B_1, known as the Swanson hump,[28] in the experimental TEDs in FE and PFE.[15–17,26,27] The calculated K-SDOS of clean W(100), plotted in Fig. 2(b), shows a peak B_1' that is due to a pair of d_{z^2}-like surface states B_1' close to $\bar{\Gamma}$ that are responsible for the observed peak B_1. States B_1' shift by about −1.2 eV [states F_1' in the energy-band diagram of W(100)/Na $c(2\times2)$ in Fig. 2(a)] due to overlap with the s-like valence states of the overlayer, and yield peaks F_1' in the K-SDOS [Fig. 2(c)] and the TED in PFE. This is consistent with the observed suppression of the experimental peak B_1 in the TED in FE from clean W(100) above a Na coverage of 0.5 ML, and the strong enhanced emission in the TED in FE and PFE (peak F_1) at 1 ML at −1.5 eV.[15] The symmetry point $\bar{M}$ in the SBZ of clean W(100) is folded back to $\bar{\Gamma}'$ in the SBZ of the

TABLE I. Comparison of the peaks observed in the experimental TEDs in FE and PFE from clean W(100) (A_1 and B_1) (Refs. 16 and 17) and W(100)/Na $c(2\times2)$ (F_1 to J_1) (Ref. 15), with peaks in the calculated TEDs. The acronym ss stands for surface states and sr stands for surface resonances.

Experimental Peak label	$E-E_F$ (eV)	Peak label	$E-E_F$(eV)	Character	Calculated Symmetry in overlayer [substrate]
A_1	-0.73 (5)	A_1'	-0.69 (2)	sr	$[d_{xz}+d_{yz}]$
B_1	-0.32 (3)	B_1'	-0.32 (2)	ss	$[d_{z^2}]$
F_1	$\leqslant -1.5$	F_1'	-1.50 (2)	ss	$s\,[d_{z^2}]$
G_1	-0.8 (1)	G_1'	-0.63, -0.83 (2)	sr	$s\,[d_{xz}+d_{yz}]$
H_1	close to $+0.0$	H_1'	$-0.05+0.04$ (2)	sr	$p_x+p_y\,[d_{xz}+d_{yz}]$
J_1	$\geqslant +1.0$	J_1'	$+1.2$ to $+1.6$	ss – sr	$p_z\,[d_{z^2}]$

overlayer [see the SBZs in Fig. 1(a)]. Since FE is dominated by the emission from electron states close to $\bar{\Gamma}'$, the emission from states at $\bar{\mathrm{M}}$ is negligible from clean W(100) but can be significant from W(100)/Na $c(2\times2)$. Peak J_1' in Fig. 2(c) results from the overlap of p_z-like states of the overlayer and d_{z^2}-like surface states of clean W(100) that have been folded back to $\bar{\Gamma}'$ from $\bar{\mathrm{M}}$. Peak J_1' is consistent with the strong peak J_1 at or above $+1.0$ eV,[15] observed in the experimental TED in FE at 1-ML coverage, whose exact energy cannot be determined due to the reduced electron occupation above E_F. Because the energies of states F_1' and J_1' differ by roughly the photon energy used, it is expected that bulk photoexcitation between these states will contribute to the strength of the experimental peak F_1.

Peaks A_1' and B_1' of clean W(100) demonstrate clearly the effect of the electron states' symmetry on the emission strength in FE. While comparable in the K-SDOS, peak A_1' is much weaker than peak B_1' in the TED in FE,[16] consistent with experiments, because the zero expansion coefficients $A_{\mathbf{k},0}$ of the $d_{xz}+d_{yz}$-like states dominating peak A_1' are much smaller than $A_{\mathbf{k},0}$ of the d_{z^2}-like states dominating peak B_1'. Overlap between Na s-like states and the surface resonances A_1' in an extended region along $\bar{\Gamma}'\bar{\mathrm{X}}'$ yields the calculated peak G_1' in PFE, consistent with the strong peak G_1 observed at a Na coverage from 0.4 to 0.8 ML[15] [see lower curve in Fig. 2(e) at 0.6-ML coverage]. Another peak D was reported in the TED in PFE at 1 ML in Fig. 4 of Ref. 15. The TED was, however, shifted erroneously in energy by $+0.5$ eV resulting

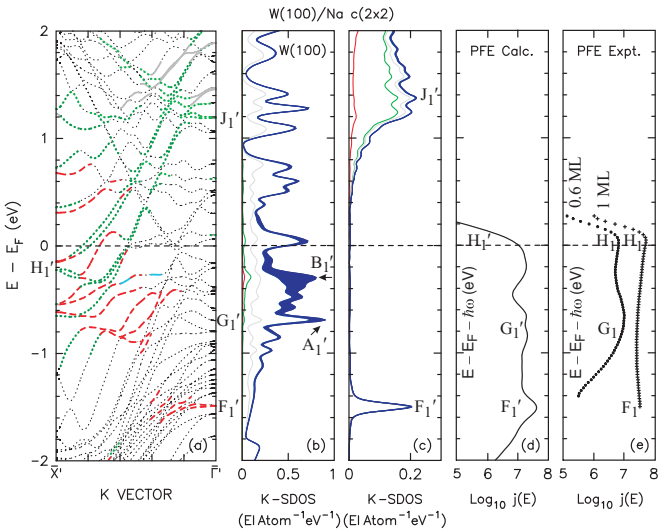

FIG. 2. (Color online) (a) Dispersion along $\bar{\mathrm{X}}'\bar{\Gamma}'$ of W(100)/Na $c(2\times2)$. Surface states and surface resonances are shown by thick curves. The predominant symmetry in the surface layer is shown by the line style [s, red (dashed); p, green (dotted); and d, blue or gray (solid)]. Bulk and intermediate states are shown by thin gray (dotted) curves. K-SDOS of (b) clean W(100) and (c) a Na $c(2\times2)$ overlayer on W(100). The successive curves in the cumulative plots (b) and (c) show the contributions of s-like (red), p-like (green), $d_{xy}+d_{x^2-y^2}$-like (gray), $d_{xz}+d_{yz}$-like (light blue), and d_{z^2}-like (dark blue) states, respectively. The shading denotes the d_{z^2}-like contributions. [(d) and (e)] TEDs in PFE for W(100)/Na $c(2\times2)$ with 3.05- eV photons, plotted as a function of the initial-state energy. $\mathrm{Log}_{10}\,J(E)$ has been displaced horizontally by arbitrary amounts. The calculated plot (d) is based on surface photoexcitation. The experimental plot (e) shows a strong peak F_1 that is due to surface as well as bulk photoexcitation.

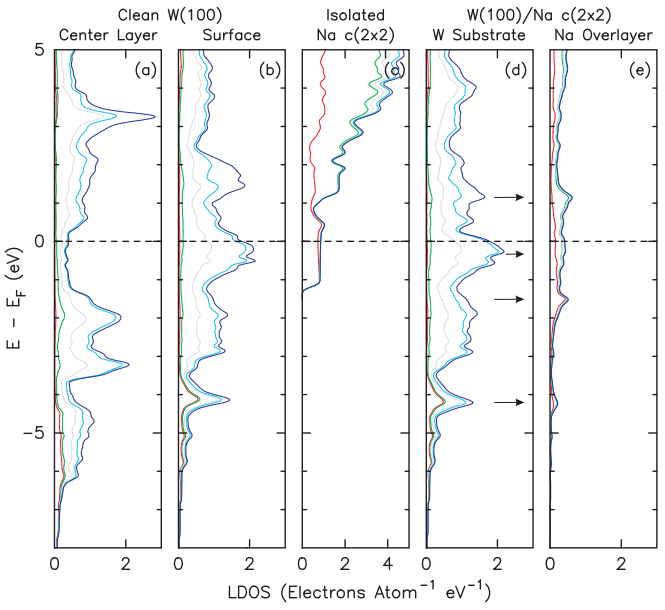

FIG. 3. (Color online) Layer density of states of clean W(100) in the (a) central (bulk) layer and (b) surface layer. (c) LDOS in an isolated Na $c(2\times2)$ layer. LDOS of W(100)/Na $c(2\times2)$ in the (d) W substrate and (e) Na overlayer. In these cumulative plots, the areas between successive curves show the contributions of s-like (red), p-like (green), $d_{xy}+d_{x^2-y^2}$-like (gray), $d_{xz}+d_{yz}$-like (light blue), and d_{z^2}-like (dark blue) states, respectively.

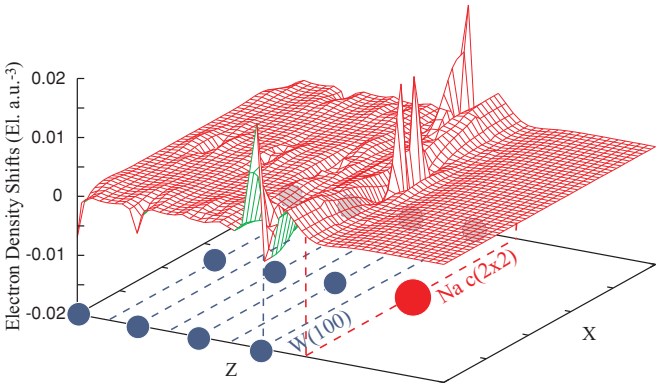

FIG. 4. (Color online) Calculated redistribution of the valence electron density that occurs when a Na $c(2 \times 2)$ overlayer is adsorbed on a W(100) surface, plotted in a {110} plane that intersects the surface at right angles. The dashed rectangles represent the planes of the overlayer (labeled Na) and of the substrate (labeled W). A positive shift corresponds to an increased electron density.

in the suggestion that peak D observed at a final-state energy at +3.2 eV was due to a high DOS at the final-state energy, i.e., due to bulk photoexcitation. According to our calculations peak D (labeled H_1 in the present work) is attributed to surface photoexcitation from bands of surface states and resonances H_1' crossing E_F [Fig. 2(a)].

In summary, our calculated results are consistent with the peaks observed in FE and PFE from clean W(100) and W(100)/Na $c(2 \times 2)$ (Table I), indicating that the present calculations give a realistic picture of the changes in the electronic structure of W(100) due to adsorption of a Na $c(2 \times 2)$ overlayer.

B. Layer densities of states and work function of W(100)/Na $c(2 \times 2)$

The SDOS of the W(100)/Na $c(2 \times 2)$ overlayer [Fig. 3(e)] deviates strongly from the nearly free-electron-like, predominantly s-like LDOS of an isolated Na layer around E_F [Fig. 3(c)], calculated using a supercell in which Na atoms occupy the same sites as in the W(100)/Na $c(2 \times 2)$ supercell and the W sites are empty. The strong surface resonance peaks in the occupied SDOS of clean W(100) at −4.1 and −0.3 eV [Fig. 3(b)] are only slightly affected [see Fig. 3(d)]. The Na charge is found to redistribute among the various symmetry components. The s-like charge within the atomic sphere of radius 1.7 Å decreases by 0.43 electrons per Na atom and the p-and d-like charges increase by 0.31 and 0.12 electrons, respectively, hence no charge transfer from the overlayer to the substrate occurs. A similar conclusion was reported[13] based on experimental photoemission measurements from W(110) with Na, K, and Cs overlayers at coverages up to one atomic layer that show little if any shifts of the energies of the core $3p$ and $4f$ W electrons.

The spatial redistribution of the valence electron density in a {110} plane that occurs when a Na $c(2 \times 2)$ overlayer is adsorbed on W(100) is shown in Fig. 4. It was obtained by subtracting the sum of the valence electron density distribution of clean W(100) and of the isolated Na $c(2 \times 2)$ overlayer from that of W(100)/Na $c(2 \times 2)$. Electrons move out from

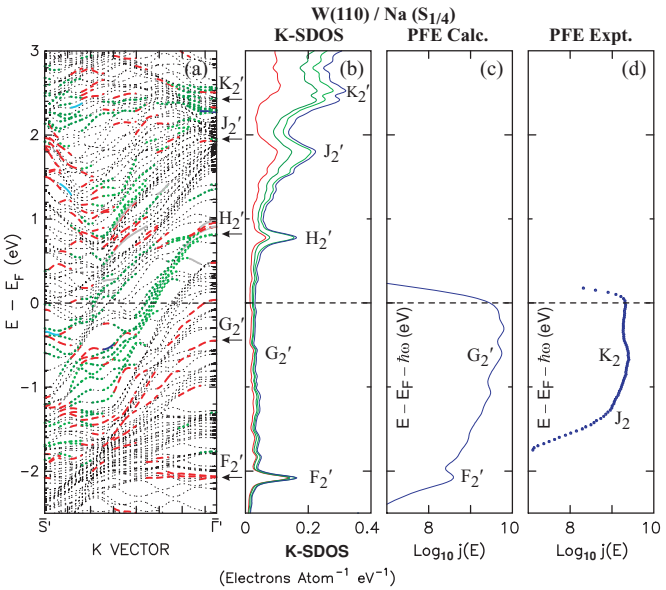

FIG. 5. (Color online) (a) Dispersion plots along $\bar{S}'\bar{\Gamma}'$ in the surface Brillouin zone of W(110)/Na ($S_{1/4}$). Interpretation of curve styles and colors are the same as in Fig. 2(a). (b) K-SDOS of W(110)/Na ($S_{1/4}$). The successive curves in the cumulative plots show the contributions of s-like (red), $p_x + p_y$-like (dark green), p_z-like (light green), and d-like (blue) states, respectively. [(c) and (d)] TEDs in PFE for W(110)/Na ($S_{1/4}$) with 3.05-eV photons, plotted as a function of the initial-state energy. $\mathrm{Log}_{10}\, J(E)$ has been displaced horizontally by arbitrary amounts. The calculated plot (c) is based on surface photoexcitation. The experimental plot (d) shows final state peaks K_2 and J_2 that are attributed to bulk photoexcitation.

the regions surrounding the W and Na atoms and accumulate in a layer between the overlayer and the substrate. The net effect is an outwardly directed dipole layer resulting in a Na-induced lowering in the potential energy of an electron outside the surface with respect to the bulk and thus lowering the work function. The work function of W(100)/Na $c(2 \times 2)$ is 2.1 eV as estimated by calculating the difference between the Coulomb potential energy far into the vacuum region of the supercell and the Fermi energy and agrees well with the value of 2.2 eV observed experimentally at 77 K using a field emission microscope,[9] and with the value of 2.3 eV calculated by means of the pseudopotential plane-wave method based on DFT.[3]

IV. RESULTS AND DISCUSSION FOR W(110)/Na

A. Field and photofield emission currents from W(110)/Na ($S_{1/4}$)

The calculated[17] and experimental TEDs[15,17,26] in FE and PFE from clean W(110) show little initial-state structure. The experimental TEDs in PFE with 3.05-eV photons in the range of coverage from $\theta = 1/7$ to $\theta = 1/4$ [Fig. 5(d)] show a strong peak K_2 that shifts slightly to lower energy with increased coverage, and that has been attributed to bulk photoexcitation.[15] At the corresponding final-state energy of +2.45 eV the K-SDOS of W(110)/Na ($S_{1/4}$) [Fig. 5(b)] shows a strong peak K_2'. Peak K_2' results from the overlap of $p_x + p_y$-like states of the isolated Na layer and d_{z^2}-like

TABLE II. Comparison between the energies of the peaks observed in the TEDs in PFE from W(110)/Na ($S_{1/4}$) (Ref. 15) and the energies of the calculated peaks.

Experimental Peak label	$E - E_F$ (eV)	Peak label	$E - E_F$ (eV)	Character	Calculated Symmetry in overlayer [substrate]
		F_2'	−2.08 (2)	sr	s [$d_{xz} + d_{yz}$]
G_2	−0.60 (3)	G_2'	−0.60 (2)	sr	s [$d_{xz} + d_{yz}$]
		H_2'	+0.80 (2)	sr	p_z [p_z]
J_2	+1.65 (3)	J_2'	+1.80 (5)	sr	s, p_z [d_{z^2}]
K_2	+2.45 (3)	K_2'	+2.5 (1)	sr	$p_x + p_y$ [d_{z^2}]

W states at +2.74 eV in clean W(110) that have been folded back from $\bar{S}$ in the SBZ of clean W(110) to $\bar{\Gamma}'$ in the SBZ of the overlayer. Peak K_2 is attributed to bulk photoexcitation between the s-like surface resonances G_2' [Fig. 5(a)] and the states K_2'. The observed TED in PFE shows another peak J_2 at 1 ML that is attributed to bulk photoexcitation to states J_2'. In Table II, the energies and symmetries of the calculated peaks in the TEDs in PFE at 3.05 eV photons [Fig. 5(c)] and the K-SDOS of W(110)/Na ($S_{1/4}$) are listed, and the energies of the peaks are compared with those observed in the PFE experiments.

The strongest peak F_2' in the calculated TED in PFE at −2.08 eV is due to the overlap of s-like states of the Na ($S_{1/4}$) overlayer and the W states to form bands of s-like surface resonances F_2' close to $\bar{\Gamma}'$. Peak F_2' could not be verified by the experimental results [Fig. 5(d)], as the involved states have energies below the cutoff due to the surface potential barrier at about −1.5 eV.

B. Layer densities of states of W(110)/Na

Peak K_2 in the experimental TEDs in PFE from W(110)/Na shifts to lower energy with increased coverage.[15] Electronic structure calculations of a metal substrate represented by a jellium model with Na overlayers arranged in a square lattice at different coverages by Ishida,[8] on the other hand, show no shift to lower energy in the SDOS of the valence states with increased Na coverage. The calculated SDOSs of W(110) in three Na overlayers of coverages $\theta = 1/6$, $1/4$, and $2/5$ at the same normal substrate/overlayer distance are shown in Figs. 6(a)–6(c). Overlap of the Na and W states results in the spreading out in energy of the SDOS and a noticeable p-like component below E_F, as is demonstrated by comparing the SDOS of W(110)/Na ($S_{1/4}$) with the LDOS of the isolated Na ($S_{1/4}$) layer [Figs. 7(e) and 7(c), respectively]. Also, slight modifications [Fig. 7(d)] in the prominent surface peaks in the LDOS of the clean substrate [Fig. 7(b)] at −3.0, −1.5, and +2.3 eV are observed. With increasing coverage, intralayer

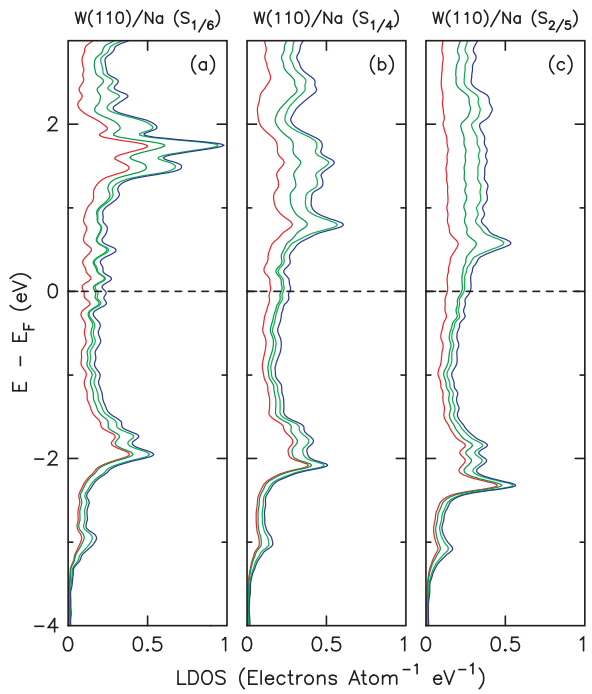

FIG. 6. (Color online) LDOS of W(110)/Na in the Na overlayer at increasing Na coverage for (a) Na ($S_{1/6}$), (b) Na ($S_{1/4}$), and (c) Na ($S_{2/5}$). In these cumulative plots, the areas between successive curves show the contributions of s-like (red), $p_x + p_y$-like (dark green), p_z-like (light green), and d-like (blue) states, respectively.

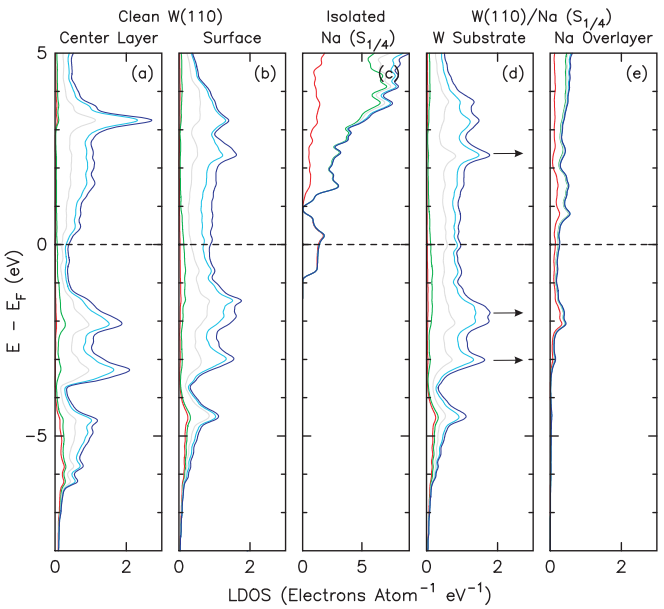

FIG. 7. (Color online) LDOS of clean W(110) in the (a) central (bulk) layer and (b) surface layer. (c) LDOS in an isolated Na ($S_{1/4}$) layer. LDOS of W(110)/Na ($S_{1/4}$) in the (d) W substrate and (e) Na overlayer. In these cumulative plots, the areas between successive curves show the contributions of s-like (red), p-like (green), $d_{xy} + d_{x^2-y^2}$-like (gray), $d_{xz} + d_{yz}$-like (light blue), and d_{z^2}-like (dark blue) states, respectively.

Na interactions broaden the peaks in the SDOS, especially above E_F, and shift the peaks to lower energy. For example, the peak below E_F that is dominated by states at $\bar{\Gamma}'$ shifts by about -0.4 eV when θ increases from 1/6 to 2/5, and the peak at $+1.7$ shifts by about -1.2 eV. Also the peak at $+2.5$ eV shifts by about -0.3 eV when θ increases from 1/4 to 2/5, in consistency with the shift to lower energy of peak K_2 in the experimental TEDs in PFE.

V. CONCLUSIONS

We interpret experimentally observed peaks in the TEDs in FE and PFE from W(100) with a Na $c(2 \times 2)$ overlayer and from W(110) with a Na (2×2) overlayer[15] by calculating the electronic structure and the TEDs of the FE and PFE currents from these interfaces. The strongest peak, the Swanson hump B_1, in the TEDs in FE and PFE from clean W(100) is suppressed due to Na adsorption. Instead a new peak F_1 is observed in the TEDs in FE and PFE from W(100)/Na $c(2 \times 2)$ due to wave function overlap at $\bar{\Gamma}'$ of the s-like valence states of the Na $c(2 \times 2)$ overlayer and the d_{z^2}-like surface states of the Swanson hump. The surface states of W(100) shift thereby by -1.2 eV.

The different symmetry of the W(100)/Na $c(2 \times 2)$ overlayer with respect to that of the clean substrate is responsible for folding back the high-symmetry point $\bar{\mathrm{M}}$ in the SBZ of the W(100) substrate to $\bar{\Gamma}'$ in the SBZ of the overlayer. This allows states at $\bar{\mathrm{M}}$ in the SBZ of the substrate to contribute to FE and PFE. d_{z^2}-like surface resonances of the W(100) substrate that have been folded back from $\bar{\mathrm{M}}$ to $\bar{\Gamma}'$ shift by about -0.5 eV due to their overlap with p_z-like conduction states of the Na $c(2 \times 2)$ overlayer. Emission from these states yields peak J_1 observed in the TED in FE from W(100)/Na $c(2 \times 2)$. A similar effect is observed when the symmetry point $\bar{\mathrm{S}}$ in the SBZ of the W(110) substrate is folded back to $\bar{\Gamma}'$ in the SBZ of the (2×2) overlayer. Bulk photoexcitation involving folded back W states is responsible for the strong peak K_2 observed in the TED in PFE from W(110)/Na ($S_{1/4}$).

There is no charge transfer from the overlayer to the substrate as we demonstrate in the case of a Na $c(2 \times 2)$ overlayer adsorbed on W(100), instead the charge is redistributed among the angular momentum states, modifying the spatial distribution of charge in the vicinity of the surface. We show that the net effect is a strong outwardly directed dipole layer resulting in a decrease in the work function. The work function we calculated for W(100)/Na $c(2 \times 2)$ is in good agreement with the experimentally observed work function at 1-ML coverage.

Contrary to Ishida's results,[8] which are based on a substrate described by a jellium model, our linear augmented plane-wave calculations show clearly that with increased Na coverage from $\theta = 1/6$ to $\theta = 2/5$ the strong peaks in the SDOS of W(110)/Na that are dominated by states at $\bar{\Gamma}'$ shift to lower energy. This energy shift is due to the increased intralayer Na interactions with increased coverage that broaden the Na states resulting in the shift of the states at $\bar{\Gamma}'$ to lower energy.

ACKNOWLEDGMENTS

This work was supported by a Natural Sciences and Engineering Research Council of Canada (NSERC) Discovery Grant. Z.A.I. wishes to thank A. I. Shkrebtii for helpful discussions during the final stages in the paper preparation.

*z.ibrahim@utoronto.ca
†Deceased.

[1] G. Furseay, *Field Emission in Vacuum Microelectronics* (Kluwer Academic/Plenum, New York, 2005).
[2] R. G. Forbes, Ultramicroscopy **95**, 1 (2003).
[3] J. Almanstötter, B. Eberhard, K. Günther, and T. Hartmann, J. Phys. D **35**, 1751 (2002).
[4] E. Wimmer, A. J. Freeman, J. R. Hiskes, and A. M. Karo, Phys. Rev. B **28**, 3074 (1983).
[5] S. R. Chubb, E. Wimmer, A. J. Freeman, J. R. Hiskes, and A. M. Karo, Phys. Rev. B **36**, 4112 (1987).
[6] P. Soukiassian, R. Riwan, J. Lecante, E. Wimmer, S. R. Chubb, and A. J. Freeman, Phys. Rev. B **31**, 4911 (1985).
[7] N. D. Lang, Phys. Rev. Lett. **55**, 230 (1985).
[8] H. Ishida, Phys. Rev. B **38**, 8006 (1988).
[9] E. V. Klimenko and V. K. Medvedev, Fiz. Tverd. Tela **10**, 1986 (1968) [Sov. Phys. Solid State **10**, 1562 (1969)].
[10] V. K. Medvedev, A. G. Naumovets, and A. G. Fedorus, Sov. Phys. Solid State **12**, 301 (1970).
[11] A. Mlynczak and R. Niedermayer, Thin Solid Films **28**, 37 (1975).
[12] A. P. Ovchinnikov and B. M. Tsarev, Sov. Phys. Solid State **9**, 1519 (1968).
[13] D. M. Riffe, G. K. Wertheim, and P. H. Citrin, Phys. Rev. Lett. **64**, 571 (1990).
[14] W. Maus-Friedrichs, S. Dieckhoff, M. Wehrhahn, and V. Kempter, Surf. Sci. **253**, 137 (1991).
[15] A. Derraa and M. J. G. Lee, Phys. Rev. B **59**, 10362 (1999).
[16] Z. A. Ibrahim and M. J. G. Lee, Phys. Rev. B **76**, 155423 (2007).
[17] M. J. G. Lee and Z. A. Ibrahim, Phys. Rev. B **70**, 125430 (2004).
[18] P. Blaha, K. Schwarz, G. K. H. Madsen, D. Kvasnicka, and J. Luitz, WIEN2k, An Augmented Plane Wave + Local Orbitals Program for Calculating Crystal Properties (Karlheinz Schwarz, Techn. Universität Wien, Austria), 2001.
[19] J. P. Perdew, J. A. Chevary, S. H. Vosko, K. A. Jackson, M. R. Pederson, D. J. Singh, and C. Fiolhais, Phys. Rev. B **46**, 6671 (1992).
[20] J. P. Desclaux, Comput. Phys. Commun. **1**, 216 (1969). **9**, 31 (1975).
[21] D. D. Koelling and B. N. Harmon, J. Phys. C **10,** 3107 (1977).
[22] A. H. MacDonald, W. E. Pickett, and D. D. Koelling, J. Phys. C **13**, 2675 (1980).
[23] D. J. Singh, *Plane Waves, Pseudopotentials and the LAPW Method* (Kluwer Academic, Dordrecht, 1994).

[24]A. Modinos and N. Nicolaou, Phys. Rev. B **13**, 1536 (1976).
[25]C. Schwartz and M. W. Cole, Surf. Sci. **115**, 290 (1982).
[26]E. W. Plummer and A. E. Bell, J. Vac. Sci. Technol. **9**, 583 (1972).
[27]Z. A. Ibrahim and M. J. G. Lee, Prog. Surf. Sci. **67**, 309 (2001).
[28]L. W. Swanson and L. C. Crouser, Phys. Rev. Lett. **16**, 389 (1966).